Regional Climate Change in East Asia Simulated by an Interactive Atmosphere–Soil–Vegetation Model

MING CHEN

Institute of Atmospheric Physics, Chinese Academy of Sciences, Beijing, China

DAVID POLLARD AND ERIC J. BARRON

EMS Environment Institute, The Pennsylvania State University, University Park, Pennsylvania

(Manuscript received 5 August 2002, in final form 12 May 2003)

ABSTRACT

A regional coupled soil–vegetation–atmosphere model is used to study changes and interactions between climate and the ecosystem in East Asia due to increased atmospheric CO_2. The largest simulated climate changes are due to the radiative influence of CO_2, modified slightly by vegetation feedbacks. Annual precipitation increases by about 20% in coastal areas of northern China and in central China, but only by 8% in southern China. The strongest warming of up to 4°C occurs in summer in northern China. Generally, the climate tends to be warmer and wetter under doubled CO_2 except for inland areas of northern China, where it becomes warmer and drier. Most of the changes discussed in this paper are associated with changes in the East Asian monsoon, which is intensified under doubled CO_2.

The largest changes and feedbacks between vegetation and climate occur in northern China. In some coastal and central areas around 40°N, temperate deciduous forests expand northward, replacing grassland due to warmer and wetter climate. Evergreen taiga retreats in the coastal northeast, causing extra cooling feedback due to less snow masking. The largest changes occur in extensive inland regions northward of 40°N, where deserts and shrub land expand due to warmer and drier conditions, and water supply is a critical factor for vegetation. These northern inland ecosystems experience considerable degradation and desertification, indicating a marked sensitivity and vulnerability to climatic change.

1. Introduction

East Asia is noted for its monsoon climate. The monsoonal circulation produces distinct seasonal and spatial patterns in temperature, precipitation, and surface hydrology. Natural vegetation varies widely over this region, and includes tropical and subtropical evergreen forests, temperate coniferous forests, semiarid woodland, grasslands, scrub tundra, and arid desert. Though soil, topography, and geomorphology influence the distribution of ecosystems in East Asia, climate is the most important driving force. Vegetation growth closely follows the seasonal cycle of monsoon circulation. It is also quite sensitive to interannual climate variability. In northern China, summer precipitation accounts for about 70% of the annual total precipitation. The interannual variability of precipitation in northern China is significant, ranging from 20% to 30% or more of annual precipitation for some areas (Ding 1994). The high interannual variability represents quite unstable climate conditions, which in turn influence ecosystems across East Asia. The satellite-derived Normalized Difference Vegetation Index (NDVI) is much higher in strong monsoon years than in weak ones (Fu and Wen 1999), suggesting that the monsoon shapes natural vegetation growth and distribution, which in turn feed back on local climate.

Global coupled atmosphere–vegetation–soil models have been developed for climate studies since the 1980s, for instance, recently by Foley et al. (1998), Dickinson et al. (1998), Wang and Eltahir (2000a), and Tsvetsinskaya and Mearns (2001). Regional studies by Lu et al. (2001) have shown that seasonal variations in phenology strongly influence climate patterns. Wang and Eltahir (2000b) proposed that the regional climate system may have multiple equilibrium states for the same forcing, and the equilibrium state is sensitive to initial vegetation distribution. Paleoclimate GCM modeling studies have suggested that atmosphere–vegetation interactions could amplify orbitally induced climate change (e.g., Texier et al. 1997). Claussen (1997) reassessed desert dynamics using a coupled atmosphere–biome model, corroborating Charney's (1975) theory of self-induce-

Corresponding author address: Ming Chen, Institute of Atmospheric Physics, Chinese Academy of Sciences, Beijing 100029, China.
E-mail: chenming@tea.ac.cn

ment of deserts. Zeng and Neelin (2000) used a coupled tropical atmosphere–land–vegetation model to explore vegetation distribution in Africa, suggesting that positive vegetation feedbacks tend to increase the gradient between desert and forest at the expense of savanna. Hoffman and Jackson (2000) found that conversion of savanna to grassland reduces precipitation by 10% over most savanna regions due to reduction in roughness length and increase in albedo. These ecosystem–climate studies have demonstrated the importance of interactions in the atmosphere–vegetation system.

Most previous studies of surface–atmosphere feedbacks in the East Asian monsoon system have focused either on the atmospheric response to prescribed surface conditions, or on vegetation responses to prescribed climatic changes. For example, Meehl (1994) used National Center for Atmospheric Research Community Climate Models (CCM0 and CCM1) and the Australian Bureau of Meteorology Research Centre (BMRC) GCM to study the influence of land surface on the Asian summer monsoon. His study showed that stronger monsoons are associated with lower land albedo, higher soil moisture, and reduced snow cover. Ferranti et al. (1999) applied their Integrated Forecast System (IFS) GCM to study the effect of surface feedbacks on monsoon circulation, finding that intraseasonal monsoon variability is enhanced by surface feedbacks. Ni (2001) estimated the future vegetation distribution and carbon storage in China using the BIOME3, process-based equilibrium terrestrial biosphere model driven by output for the end of the twenty-first century from the Hadley Centre coupled ocean–atmosphere general circulation model. He concluded that elevated CO_2 concentrations will produce an increase in carbon storage in vegetation and soils, due mainly to increases in vegetation area induced by the changing climate; furthermore, the finer the spatial resolution in mapping vegetation, the better the estimate of carbon storage. All these studies have been performed using one-way coupling, without any consideration of interactive feedbacks between ecosystem and atmosphere. However, vegetation is intrinsically an interactive component in the climate system. Interactive climate–ecosystem models are needed to advance our understanding of variability and trends in climate.

Ecosystem–climate interactions vary between regions. Several models have found unique factors in the East Asian monsoon climate. For example, in their soil moisture–precipitation sensitivity experiments, Shukla and Mintz (1982) found that precipitation increased everywhere under wet soil conditions, except in the East Asia monsoon region where precipitation decreased. Several modeling studies have shown that surface hydrology is an important interactive component in monsoon circulation development and variability (Webster and Yang 1983). Surface moisture flux is not simply determined by soil physics and atmospheric conditions; interception of precipitation and transpiration by vegetation are also important components. In addition, East Asia has a complex topography, which induces mesoscale circulations strong enough to modify synoptic circulation and form small-scale climate and vegetation characteristics, thereby causing large spatial variance. Some mesoscale processes that are important for regional climate and vegetation evolution are not well represented in GCMs. Further knowledge of interactions between climate and ecosystem in East Asia is limited. Thus it is important to apply higher-resolution models in East Asian studies.

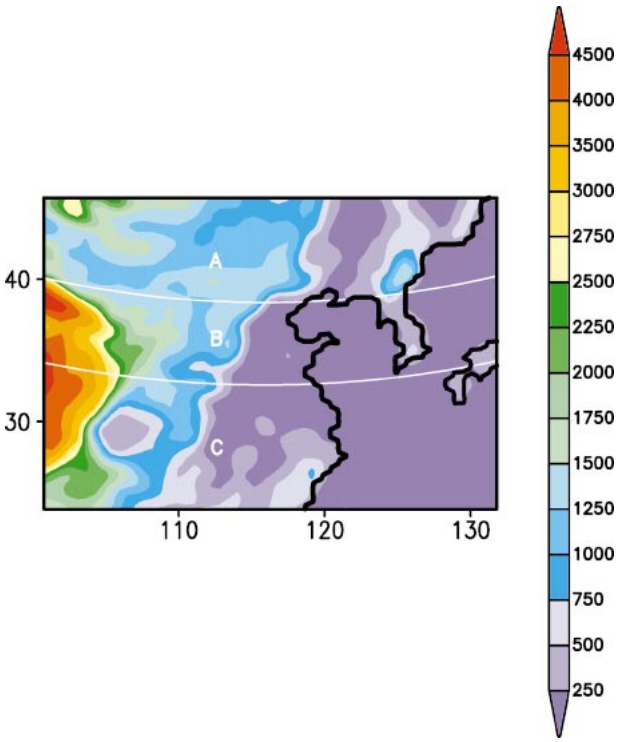

FIG. 1. Regional model domain, topography (m), and three subregions divided by east–west lines for which spatial averaged results are discussed in the text: A ≡ northern China; B ≡ central China; C ≡ southern China.

In this study, a regional coupled soil–vegetation–atmosphere model is applied to East Asia, focusing on climate change and interactions between climate and ecosystem. Brief descriptions of the atmospheric model MM5, land surface model LSX and equilibrium biosphere model BIOME are given in the next section, and the experimental design is described in section 3. Present-day climate results are shown in section 4. Changes due to doubled CO_2 with fixed vegetation are described in section 5, and section 6 discusses vegetation changes and climate–vegetation feedbacks with interactive vegetation. A summary and conclusions are given in section 7.

2. Model description

This study uses a coupled regional model that includes interactions between the atmosphere, surface

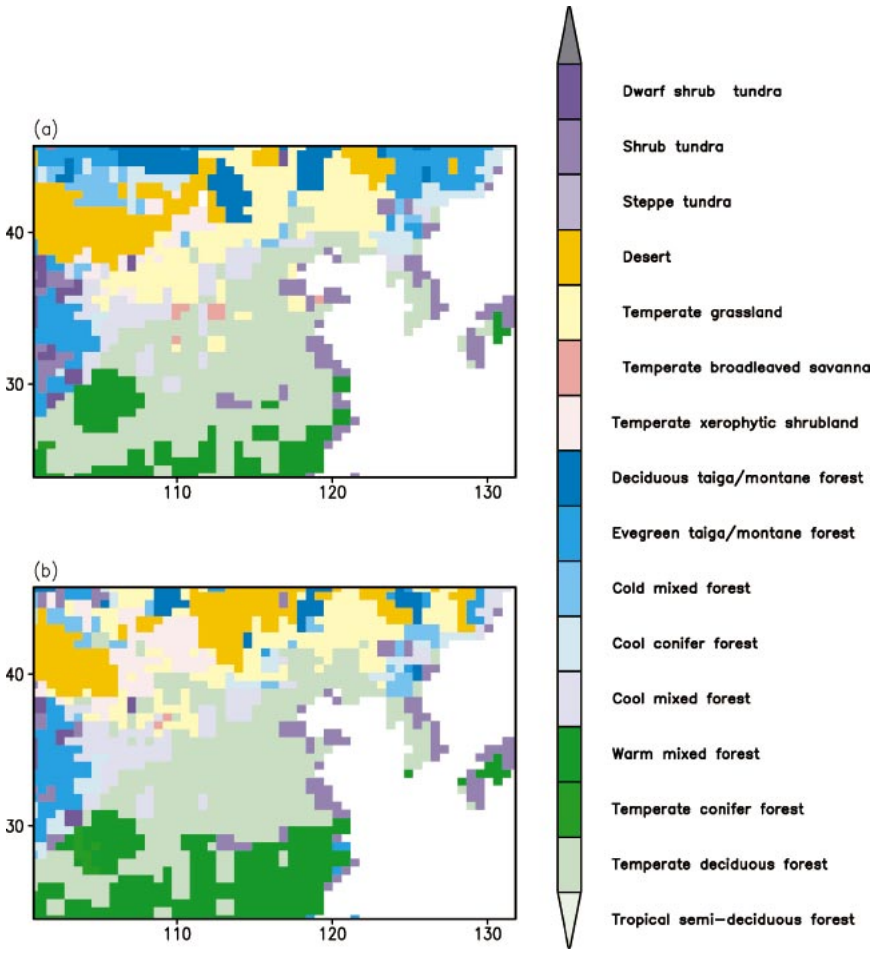

FIG. 2. Vegetation distribution predicted by BIOME4. (a) Forced by modern observed climatology, specified for runs CTRL and RUN2. (b) For doubled CO_2 in the MM5 regional model with interactive vegetation (RUN3, year 8).

physics, and vegetation. The atmospheric component is based on the fifth-generation Pennsylvania State University–National Center for Atmospheric Research Mesoscale Model (PSU–NCAR MM5; Grell et al. 1994), a nonhydrostatic primitive equation model written in terrain-following sigma coordinates, originally developed for medium-range forecasting. In order to make it applicable for long-term simulations, some important modifications have been made.

To simulate surface processes on long time scales, the Land Surface Transfer scheme (LSX) is coupled with MM5. LSX is a detailed surface model describing soil, snow, and canopy physical processes, used in the Global Environmental and Ecological Simulation of Interactive Systems (GENESIS) global climate model (Thompson and Pollard 1997; Pollard et al. 1998). A detailed formulation of LSX is given in Pollard and Thompson (1995). Functioning as a link between the regional climate model and surface soil and snow models, it computes exchanges of momentum, thermal energy, and water mass between atmosphere and land surface, given current atmospheric conditions above and current soil and snow conditions below. Intercepted liquid and snow and the cascade of precipitation through the two-story canopy are also predicted. Fluxes in radiation, sensible heat, and water vapor above the upper canopy are passed to the atmospheric model. Similarly, net downward fluxes of heat and water at ground level are passed to multilayer soil and snow models.

As an important interface between soil and atmosphere, the equilibrium vegetation model BIOME (Haxeltine and Prentice 1996) is interactively and asynchronously coupled with the model system. BIOME is particularly suitable for predicting changes in natural vegetation patterns due to changes in climate since it is based on physiological considerations rather than on correlations between climate and vegetation as they exist today. When driven by modern observed climatology, BIOME successfully reproduces broad-scale patterns of potential vegetation distribution (Haxeltine and Prentice 1996). BIOME model's ability to quickly compute equilibrium vegetation conditions makes it espe-

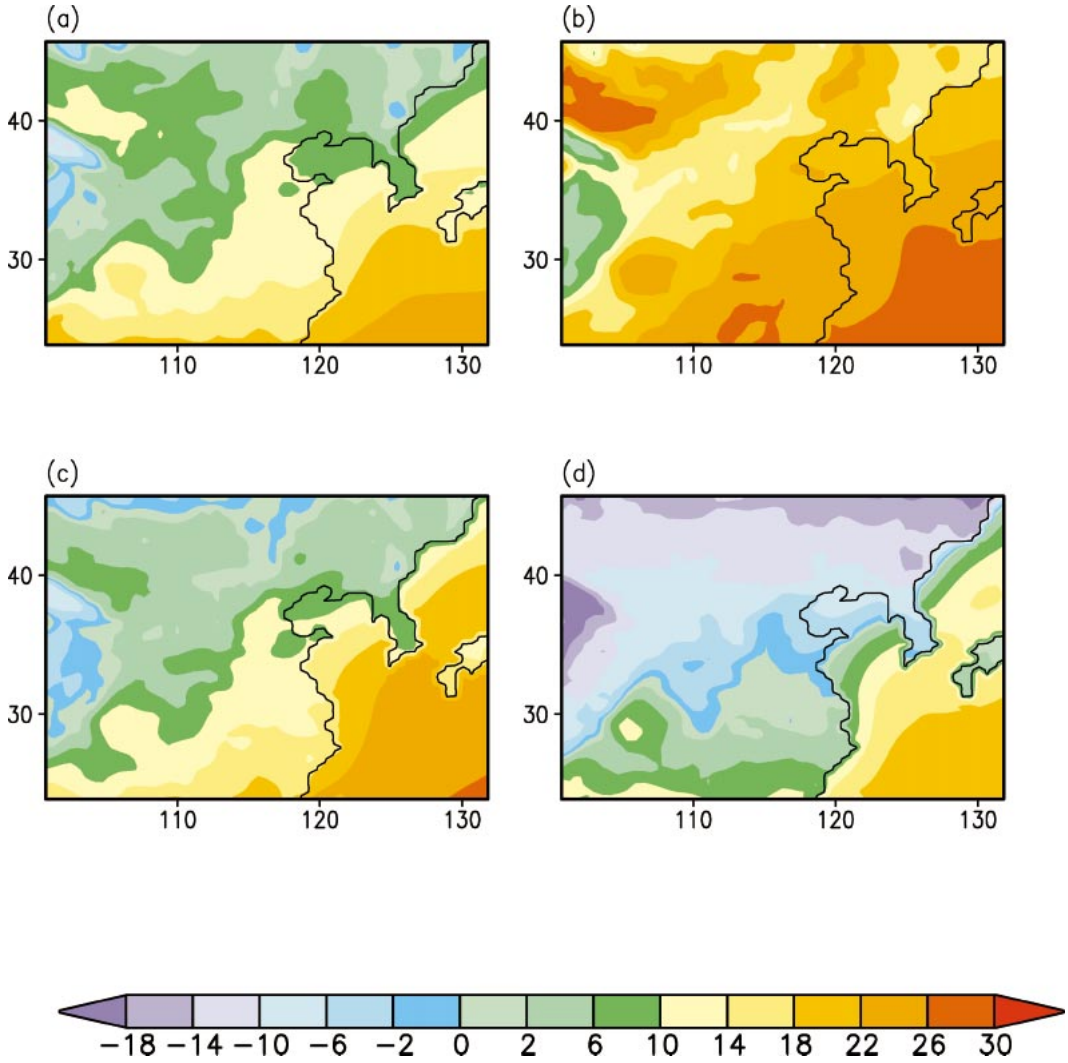

FIG. 3. Seasonal surface air temperature (°C) for the present in the MM5 regional model (CTRL): (a) spring [Mar–May (MAM)], (b) summer [Jun–Aug (JJA)], (c) autumn [Sep–Nov (SON)], and (d) winter [Dec–Feb (DJF)].

cially suitable in regional climate–ecosystem interaction studies. Furthermore, BIOME accounts the effects of doubled CO_2 in vegetation physiology and biophysics, so the vegetation responds to both CO_2 fertilization and CO_2-induced climate change. In this study we use the BIOME4 version, which includes improved diversity of biome types and updated process formulations and parameters (Kaplan 2001; Cramer 2002).

Realistic ocean boundary conditions have been added to MM5, with prescribed seasonally varying SSTs from the NCAR Climate System Model (CSM) GCM output (discussed later). A simple slab water model is used in MM5/LSX to describe inland water bodies. Other choices of physical schemes within MM5 are Grell et al.'s (1994) cumulus parameterization scheme, the simple ice scheme (Dudhia 1989), CCM2 radiation scheme (Briegleb 1992), and the medium-range planetary scheme (Hong and Pan 1996).

3. Regional model domain and experiment design

The MM5 regional model domain is centered on (36°N, 116°E), covering a region in East Asia roughly 3900 km by 3120 km with a grid interval of 60 km. The model has 16 levels in the vertical, with higher resolution in the planetary boundary layer below 1500 m, and with the model top at 100 mb. Prescribed topography is shown in Fig. 1, along with three subregions with distinct climate regimes for which spatially averaged results are presented in later sections. All averages are calculated just over land points, excluding ocean.

To assess the impact of increasing greenhouse gas on climate and ecosystems in the East Asian monsoon region, and also the two-way interaction between climate and vegetation, three MM5 experiments have been performed, each 8 yr in length: 1) a present-day control run with potential vegetation specified by BIOME4 driv-

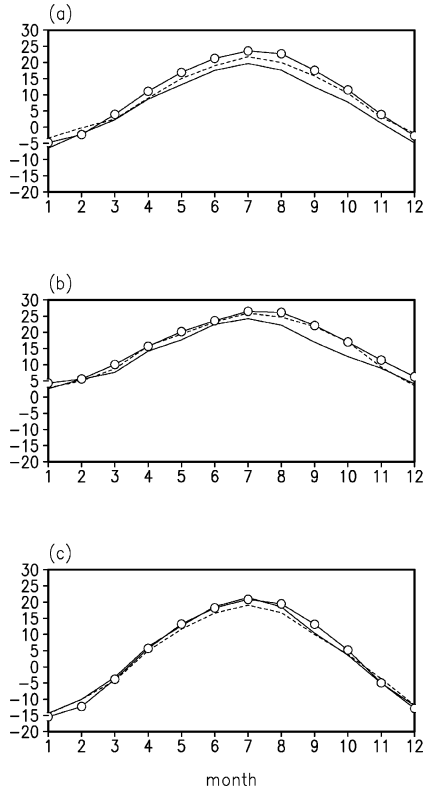

FIG. 4. Seasonal cycles of surface air temperature (°C) for the present, averaged over land for the three subregions shown in Fig. 1: (a) northern China, (b) central China, (c) southern China. Solid lines are for the CSM GCM, dashed lines for the MM5 regional model (CTRL), and circles are for observed climatology (CRU dataset, 1961–90; New et al. 1999).

en by present observed climatology (CTRL); 2) a ''doubled CO_2'' run with the same vegetation distribution as in the control run (RUN2); and 3) a doubled CO_2 run with interactive BIOME4 vegetation (RUN3). In RUN3, asynchronous coupling is used as in Claussen (1994), except that BIOME4 is run at the end of each year using anomalies from the regional model (differences of monthly mean temperature, precipitation, and cloudiness from the control run, RUN3 − CTRL) superimposed on present observed climatology (Leemans and Cramer 1991). The integrations are run for eight successive years to allow the climate–vegetation system to reach equilibrium in RUN3 (Texier et al. 1997; Claussen 1997). As discussed later, differences between RUN3 and RUN2 will show the impact of vegetation–climate feedbacks for increased CO_2. The BIOME4 vegetation distribution specified for the noninteractive runs (CTRL, RUN2) is shown in Fig. 2a; for ease of comparison, Fig. 2b shows the vegetation in the interactive doubled CO_2 run (RUN3), discussed further later. All results are averaged temporally over the 8 yr of each model run.

Large-scale forcing from a 145-yr transient archived simulation of the CSM GCM (Boville and Gent 1998) is used to drive the regional model. In that archived simulation, CSM was run at T42 horizontal spectral resolution with 18 hybrid-sigma levels in the vertical. It was spun up with present conditions for 15 yr, and for the next 10 yr (years 15–24) CO_2 was held constant at its present level. From year 25 on, CO_2 was increased at 1% yr^{-1}. CO_2 doubling was achieved in year 95. CSM outputs for years 15–22 and years 95–102 are used as the driving fields for regional model integrations. Throughout this paper the former experiments are termed ''present,'' and the latter are termed 2090s or doubled CO_2, even though CO_2 was not exactly double over the decade. Lateral boundary conditions are provided at 6-h intervals and linear time interpolation is performed at intervening time steps. A dynamic relaxation technique (Newtonian nudging and horizontal diffusion; Davies and Turner 1977) is applied in the regional model buffer zone. Linear-decay relaxation coefficients (Grell et al. 1994) are adopted. Regional model results are evaluated below against National Centers for Environmental Prediction (NCEP)–NCAR 40-year Reanalysis Project (NNRP) reanalysis data (Kalnay et al. 1996), Climate Research Unit (CRU) 1961–90 observed climatology (New et al. 1999), and CSM output. Note that there are errors at a few individual stations in the CRU dataset, with varying significance depending on the density of the surrounding network. Where the network is sparse, a station error influences a larger area because of its greater spatial influence during interpolation (New et al. 1999). Due to the complex terrain in East Asia, large discrepancies exist between various datasets, although they are all based on observations. For instance, precipitation in the Xie and Arkin (1996) dataset (not shown) is larger than that from CRU in almost all seasons. In this study we use CRU to compare with our model results because its spatial resolution (0.5°) is relatively close to that of the regional model (60 km), compared to 2.5° for Xie–Arkin. It should be noted that the 6-h GCM forcing does not correspond to actual weather sequences, so the model results are comparable to observations only as climatological averages.

The experiments in this paper are designed to answer the following questions:

1) What are the climatic changes caused by doubled CO_2 in the East Asia monsoon region simulated by a high-resolution regional climate model?
2) How will the ecosystem be reshaped under doubled CO_2 and changed climate in East Asia?
3) What role does vegetation feedback on atmosphere play in East Asian climate change in a doubled CO_2 climate?

4. Present climate

a. Temperature

Figure 3 shows seasonal (3-month average) temperatures for the control simulation. The spatial patterns of temperatures on regional scales are realistic. The center

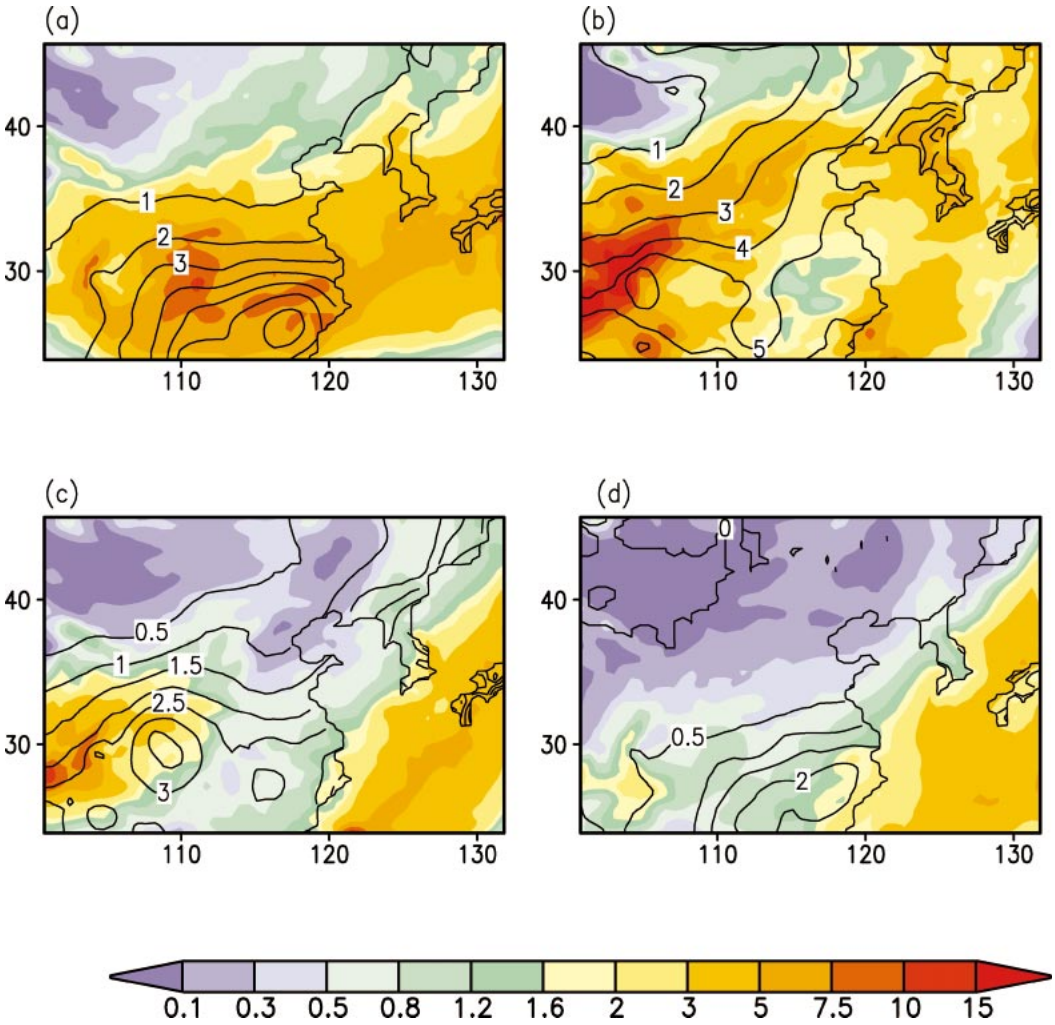

FIG. 5. Seasonal precipitation (mm day^{-1}) for the present: (a) spring (MAM), (b) summer (JJA), (c) autumn (SON), and (d) winter (DJF). Color fill represents the MM5 regional model (CTRL), and black contours represent the observed climatology (CRU dataset, 1961–90; New et al. 1999).

of high temperature in the low basin of Si Chuan province, the strong temperature gradient along the mountains extending from northeastern to southwestern China and on the eastern edge of the Tibet Plateau, and some local warm and cold centers in northern China corresponding to local high and low topography, are all well simulated.

To further evaluate the model's present-day performance, the seasonal cycles of surface temperature in the regional model, the CSM GCM, and CRU climatology are compared for each subregion (Fig. 4). In general the regional model temperatures are reasonably consistent with the observations. The CSM underestimates temperature in most seasons over all three subregions by -2° to -7°C. The regional model reduces the errors but cannot completely eliminate them in central and northern China. In southern China, the regional model underestimates temperatures in summer. Model biases in temperature are partly due to the complex terrain in East Asia, where topography rises from east to west in three distinct grades. In between are ridges, valleys, and basins on small to regional scales. They form one of the most complex terrain areas in the world and induce strong micro- and mesoscale circulation (Cai and Zhang 1978; Tao 1979). Local weather and climate are strongly influenced by these small-scale circulations, which are not resolved by the coarse resolution of several hundred kilometers in the CSM.

b. Precipitation

Seasonal precipitation is shown for the control experiment and for the observed CRU climatology in Fig. 5. The basic characteristics of monsoon precipitation in East Asia is captured by the regional model. Concentrations of heavy precipitation in southeastern China in the spring,

and in Korea and Japan in the summer are simulated correctly. The precipitation gradient from southeast to northwest is also well described. In spring the monsoon rain belt is located correctly in southern and southeastern China. The polar front forms between cold air from the north and warm moist air from the tropical and subtropical ocean, causing heavy precipitation in southern and southeastern China (Fig. 5a). With summer approaching, southerly winds advance northward and the rain belt moves to central and northern China. Monsoon circulation extends further north in late summer, and the rainy season in northern China extends from late July to early August. Korea and northeastern China become centers of rainfall in summer (Fig. 5b). The summer monsoon reaches its peak development and most northerly position in August, and then retreats rapidly. Its southward retreat is much faster than its northward advance and is unsteady, thereby preventing it from sustaining precipitation over specific regions. Starting in September, most areas of mainland China experience a dry and cloudless autumn, and precipitation concentrates in southwestern China (Fig. 5c). In winter most precipitation occurs along the coast of southern China.

Although the model precipitation is by and large realistic, some discrepancies remain. Precipitation is overestimated in central China in spring, and underestimated in southeastern China in summer. Precipitation is underestimated in southeastern China in autumn and winter. The large-scale 500-mb circulation (Fig. 6) in the CSM GCM shows that the west Pacific subtropical high is located northeast of its true position in summer, leaving most of southeastern China under the weak influence of disturbances along the monsoon front. Furthermore, the CSM 850-mb wind field (not shown) suggests that the low-level southwest wind, which is the most important component of the summer monsoon, is underestimated by CSM and causes much less water vapor transport and less precipitation. The summer monsoon in CSM advances northward earlier, and then retreats southward quicker than observed (not shown), causing overestimation of precipitation in central China in spring and underestimation in autumn. These synoptic errors in the large-scale forcing are introduced into the regional model and cause underestimation of summer precipitation. Errors in the regional model's local physics schemes may also contribute to its precipitation biases.

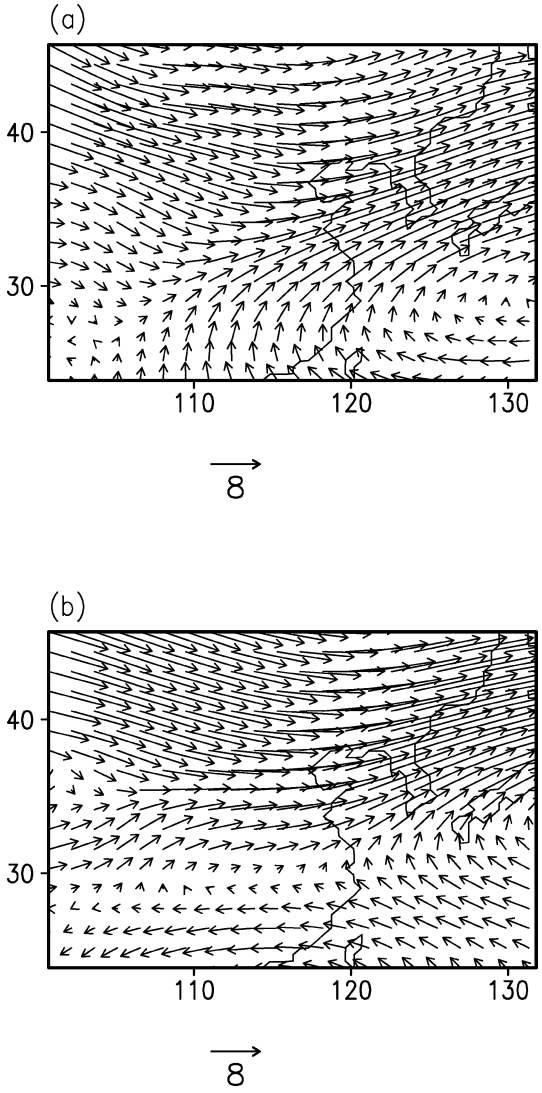

FIG. 6. The 500-mb winds in Jul for present day: (a) observed climatology (NNRP), (b) CSM GCM (Kalnay et al. 1996).

5. Changes under doubled CO_2 with fixed vegetation

a. Changes in temperature

Figure 7 shows seasonally averaged temperature changes in the 2090s doubled-CO_2 fixed-vegetation experiment (RUN2) from the present experiment (CTRL). The warming is between 1° and 4°C year-round, except for southern China in spring, where it is less than 1°C. Northern China and adjacent Mongolia experience the largest warming in summer. In winter the largest warming occurs over Tibet and the eastern part of south-central China, probably due to reduction of snow cover and albedo feedback. These large-scale patterns are similar to those of CSM (Fig. 8), although the regional model offers more spatial details. The only exception is in northeastern China, where CSM predicts strong warming (3°C) in winter.

Temperature changes are closely related both to synoptic circulation patterns and to local physical processes. The following brief analysis is similar to the more detailed discussion in Chen et al. (2003a). Under doubled CO_2, the largest precipitation increase occurs in southern China in the spring (Fig. 9a). Greater precipitation and higher soil moisture cause more evaporation, which has a strong cooling effect on the surface. Thus,

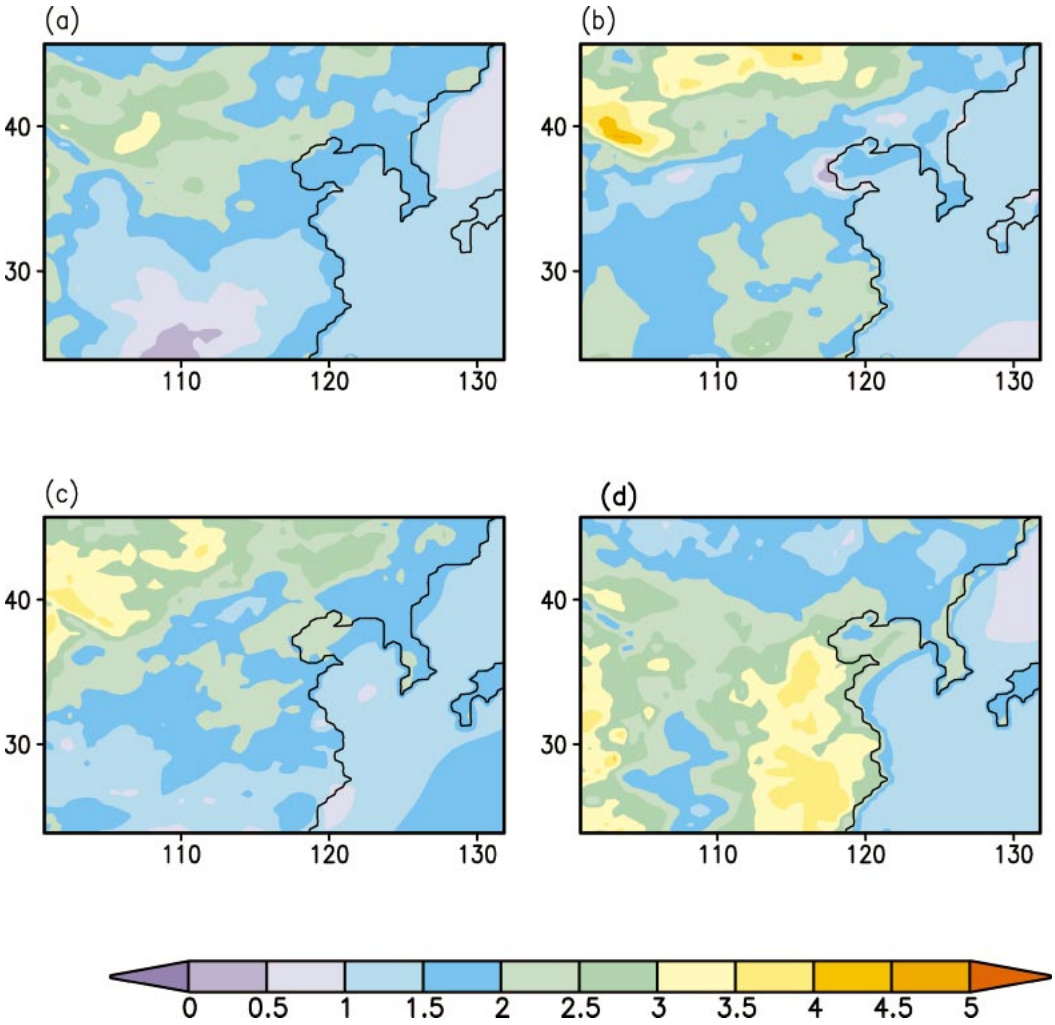

FIG. 7. Change in seasonal surface air temperature (°C) for doubled CO_2 compared to the present predicted by the MM5 regional model with fixed vegetation (RUN2 − CTRL): (a) spring (MAM), (b) summer (JJA), (c) autumn (SON), and (d) winter (DJF).

the temperature increases in the southern China spring are depressed by increased soil moisture and evaporation, and also by less solar radiation due to increased cloud cover (not shown). In northern China the opposite occurs, with very little changes in precipitation allowing greater summertime warming. In the semiarid inland region where potential evaporation is much higher than precipitation, changes in summer monsoon precipitation have important effects on the water budgets. In this situation, with little precipitation and soil moisture change, surface temperature responds strongly to the basic greenhouse gas warming.

b. Changes in precipitation

Figure 9 shows seasonally averaged precipitation changes in the 2090s fixed-vegetation experiment compared to the present (RUN2 − CTRL). The largest precipitation increases occur in spring along two east–west trending belts in southeastern and central China. These precipitation increases are due mainly to a stronger summer monsoon. In the present climate, monsoon precipitation is limited to southern China in the spring as shown in Fig. 4. With doubled CO_2, however, land heating is faster and stronger, and heating is stronger in higher latitudes, serving to increase the meridional land–sea temperature gradient. Consequently the summer monsoon strengthens in the south and the East Asia jet weakens in the north, as reflected in the wind fields at 850 mb (not shown) and 500 mb (Fig. 10a). Monsoonal circulation is stronger and reaches further north under doubled CO_2, which explains the precipitation change in the spring. In summer, there is a distinct increase in summer monsoon strength caused by a larger sea–land temperature gradient with doubled CO_2. The west Pacific subtropical high intensifies, associated with

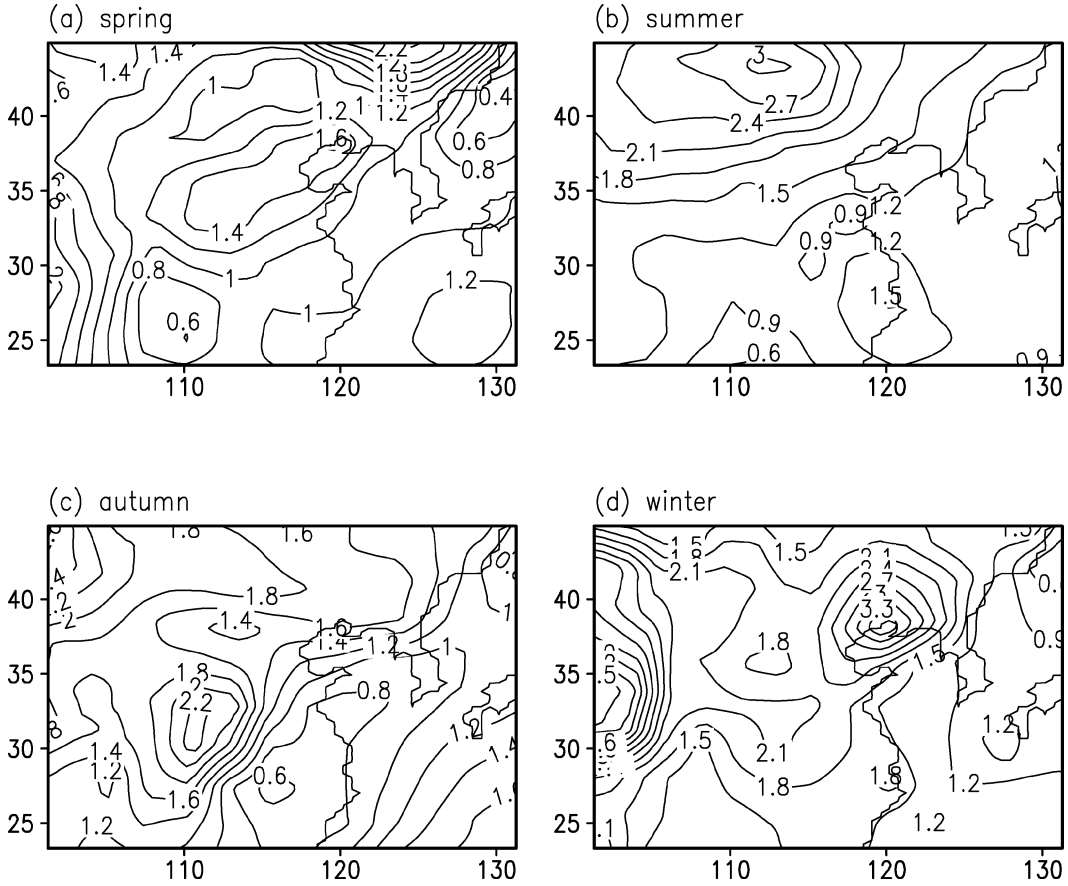

FIG. 8. Change in seasonal surface air temperature (°C) for doubled CO_2 compared to the present predicted by the CSM GCM: (a) spring, (b) summer, (c) autumn, and (d) winter.

a more vigorous meridional circulation (Fig. 10b). Southerly winds from the tropical and subtropical oceans strengthen, resulting in precipitation increases over nearly all land areas north of 30°N, with strongest increases in central regions. In northern China, precipitation increases significantly only in limited coastal areas, while most inland areas in the north and northwest experience relatively small changes. A small area in southeastern China receives less precipitation in summer due to the intensified subtropical high.

c. Changes in seasonal cycles

The seasonal cycles of temperature and precipitation changes (RUN2 − CTRL) are shown for the three subregions in Fig. 11. In southern China, precipitation increases mainly in March and September by more than 20%, but does not change much in other months except for a decrease of 18% in November. Central and northern China experience precipitation increases of 10%–40% in most months. Especially large increases occur in October in central China and in February–March in northern China, when precipitation increases by more than 50%. Averaged from May to August, precipitation increases about 25% in northern China and 28% in central China. Considering that summer is the main rainy season in central and northern China, this represents a great increase in water supply over these regions. Surface warming is strong in summer in northern China and in winter in southern China. Temperature increases are less than 2°C in southern China over the warm half-year, while stronger warming occurs in winter months. In central and northern China, the largest temperature increases occur in the transitional months of March and September. Summer warming is stronger in northern China than in central China.

6. Changes under doubled CO_2 with interactive vegetation

a. Vegetation response to climatic change

Climate variability is greater in northern China than in southern China (Ding 1994). Its larger intraseasonal and interannual variability makes the ecosystem in northern China unsteady and climatically sensitive. On the one hand, vegetation growth is vulnerable due to climate anomalies; on the other hand, the monsoon cli-

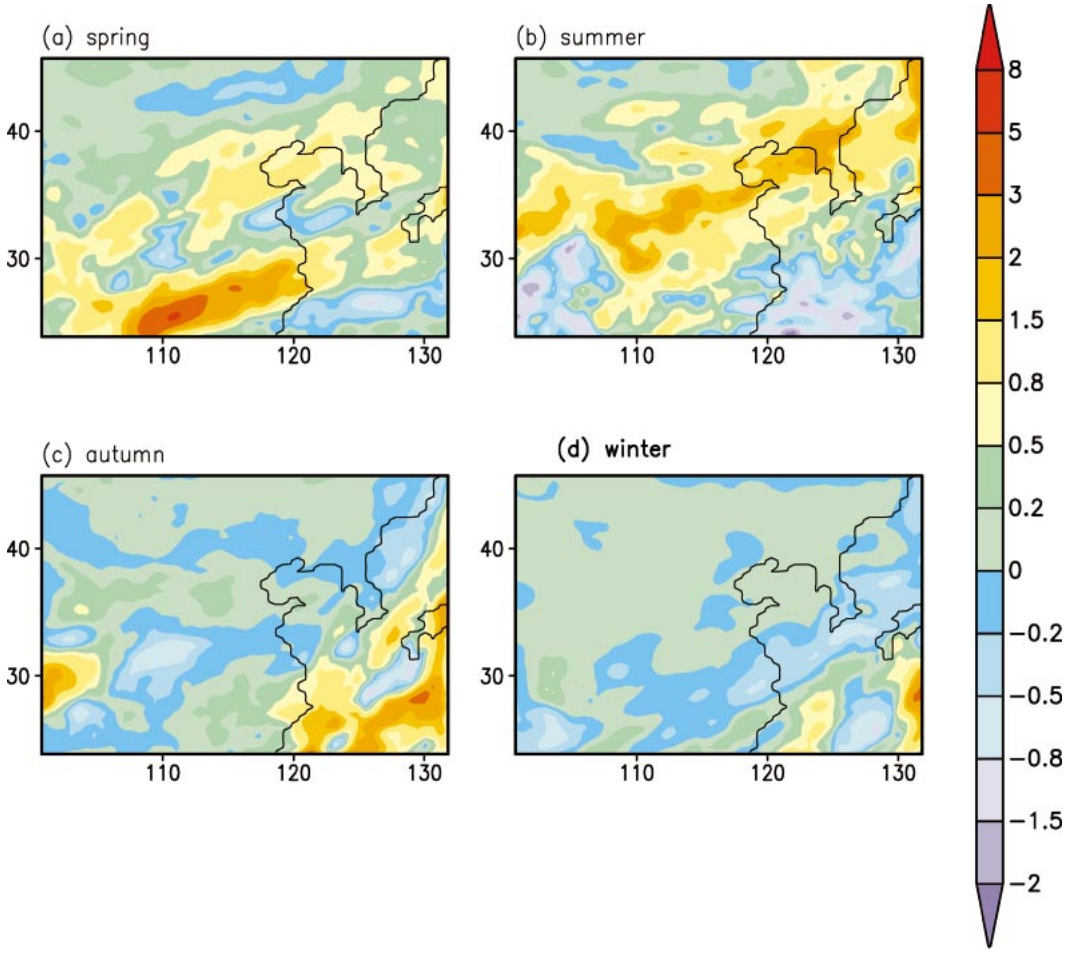

FIG. 9. Change in seasonal precipitation (mm day^{-1}) for doubled CO_2 compared to the present predicted by the MM5 regional model with fixed vegetation (RUN2 − CTRL): (a) spring (MAM), (b) summer (JJA), (c) autumn (SON), and (d) winter (DJF).

mate in East Asia is especially sensitive to land–surface feedback. Climate variability may be influenced by anomalies in synoptic circulation as well as by the anomalous state of land surface conditions. They are closely related and interact with each other. In this section we discuss the interaction and feedback between climate and vegetation in a doubled-CO_2 climate, to explore how climate change induced by increasing greenhouse gas will reshape the vegetation in monsoon China, and how the redistribution of vegetation type further feedback to climate change caused by doubled CO_2. This is done by contrasting the doubled CO_2 changes in RUN3 (with interactive vegetation) with those in RUN2 (with fixed vegetation).

Table 1 shows the fraction of grid points where vegetation type changes in successive annual iterations in the RUN3 simulation. It shows rapid and extensive initial adjustments, affecting 36% of the total area in the first year, and later the year-to-year vegetation changes due to interannual variability, which affect around 10% of the area. A similar range (10%–12%) was obtained by Texier et al. (1997) as a result of vegetation feedbacks and ineranual variability.

Figure 2b shows the vegetation distribution after the eighth year of integration in RUN3, representing the quasi-steady vegetation state in a doubled CO_2 climate. Compared with the present vegetation (Fig. 2a), most changes occur in northern China, which as noted earlier is particularly climatically sensitive and ecologically vulnerable. In a doubled CO_2 climate, forest cover decreases by 14%, shrub land and grassland areas increase by 8% and 1%, respectively, and desert increases by 4%. Shrub land and desert increase at the expense of forest and grassland, and grassland increases at the expense of forest. In the absence of other external forcing, the vegetation response to doubled CO_2 climate change in northern China involves increases of desert, grassland, and shrub land, and decreases of forest. In southern China, however, between 110° and 120°E (excluding vegetation change caused by a warmer Tibet), the main change in vegetation is the northward extension of warm mixed forest.

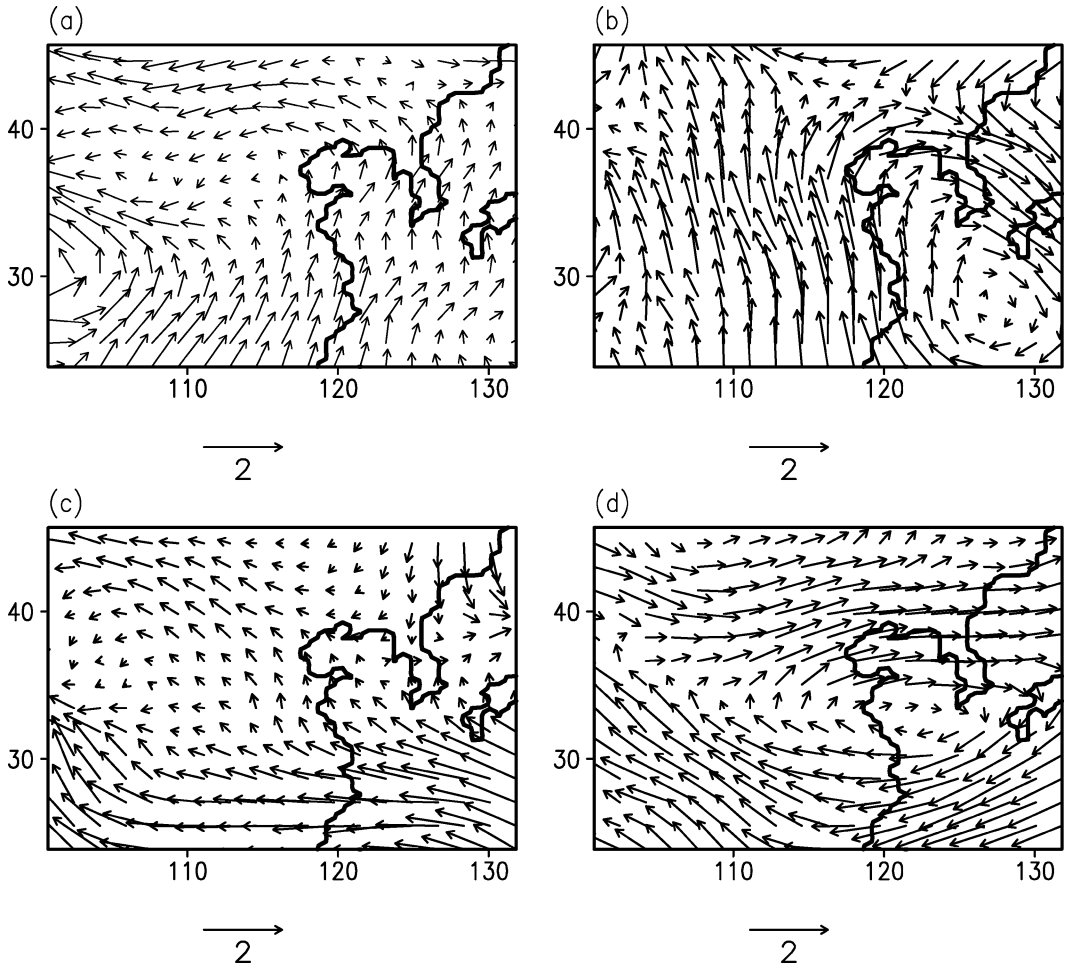

FIG. 10. Change in seasonal 500-mb wind field (m s^{-1}) for doubled CO_2 compared to the present predicted by the MM5 regional model with fixed vegetation (RUN2 − CTRL): (a) spring (MAM), (b) summer (JJA), (c) autumn (SON), and (d) winter (DJF).

The large systematic changes of vegetation in northern China, despite relatively large natural climate variability, imply a strong sensitivity in that region. Shrubland shifts northwestward and replaces the desert in the northwestern inland area, indicating the presence of more favorable conditions for vegetation growth there. In coastal and central areas around 115°–120°E at ~40°N, temperate deciduous forest expands a few degrees northward replacing grassland, due to warmer and wetter climate (Figs. 7, 9). The largest changes in the north, however, occur inland as desert replaces forest and grassland across much of the domain above 40°N, indicating a widespread deterioration of the ecosystem under doubled CO_2. Since the main growing season in northern China is late spring and early summer, these changes are not surprising given the climate changes in this region. Despite the higher temperatures (Figs. 7a,b) due to doubled CO_2 that favor vegetation growth in spring and summer in northern China, precipitation plays a more important role. As mentioned previously, potential evapotranspiration is much higher than precipitation in northern China over the entire year. Therefore water supply is critical for vegetation growth in this region. Precipitation increases slightly in spring and summer in some areas of northern China, which helps explain the northwestward expansion of shrub land there. However, in the area north of 40°N between about 110° and 120°E, spring precipitation decreases by up to 0.5 mm day^{-1} (Fig. 9), producing a 40% drop in total spring precipitation (Fig. 5). With such a large precipitation decrease, water supply becomes insufficient for vegetation growth. To make matters worse, higher temperatures in spring and summer due to doubled CO_2 cause more evapotranspiration and further intensify the drying. This explains why desert expands northward and grassland and forest recede in northern inland China.

b. Climatic response to vegetation change

Two basic vegetation quantities that influence climate are vegetation type and leaf area index (LAI). Vegetation type determines physical attributes such as fractional

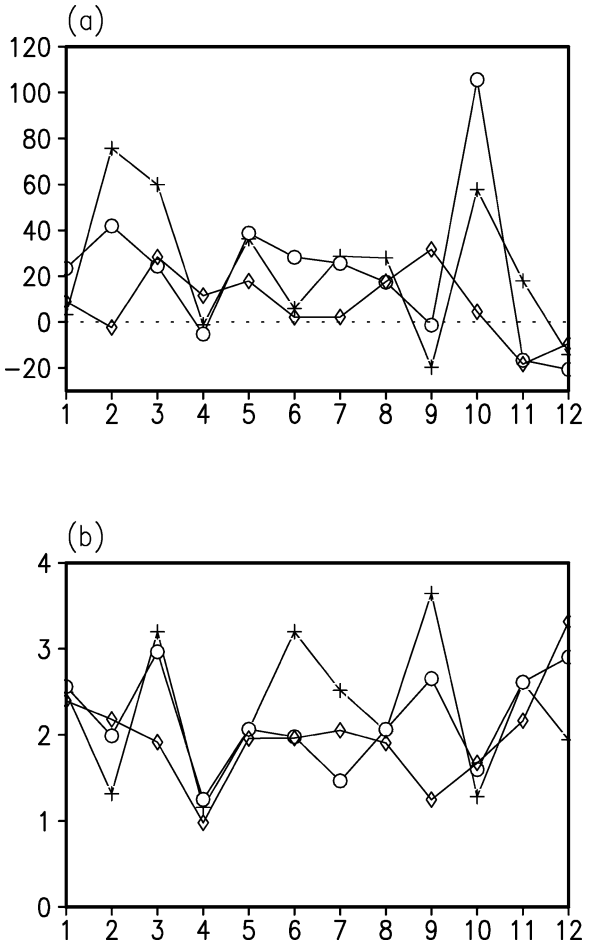

FIG. 11. Changes for doubled CO_2 compared to the present predicted by the MM5 regional model with fixed vegetation (RUN2 − CTRL), over land for the three subregions shown in Fig. 1: (a) change in monthly mean precipitation (%), (b) change in surface-air temperature (°C). Crosses are for northern China, circles for central China, and diamonds for southern China.

cover and leaf transmittance, orientation, and photosynthetically active radiation (PAR) coefficients. LAI influences canopy thickness and total amounts of transpiration and light extinction. They work together to determine water and energy exchange among soil, vegetation, and atmosphere, and to produce feedbacks on regional climate as the vegetation changes.

Figure 12 shows seasonal temperature changes due solely to vegetation–climate feedback with doubled CO_2; that is, the difference between RUN3 (interactive vegetation; Fig. 2b) and RUN2 (fixed vegetation; Fig. 2a). The most distinct differences occur in northern China. Vegetation feedbacks lead to temperature changes with amplitudes of more than 0.5°C over most areas in northern China, especially in the summer when temperatures can be up to 2°C higher in RUN3 than in RUN2.

The widespread additional summertime warming in northern inland China due to vegetation feedback (Fig. 12) mainly reflects reductions in vegetation cover and LAI, as forest and grassland are replaced by desert and shrub land (Figs. 2a,b). Much the same warming is seen in Amazonia in deforestation experiments (Lean and Rowntree 1997; Costa and Foley 2000), due to (i) reduced interception of precipitation by the canopy and less reevaporation and precipitation recycling, and (ii) greater runoff due to more intense rainfall reaching the surface, leading to drier soils, less latent heat flux, and warmer surface temperatures.

TABLE 1. Fraction of land grid points where vegetation type changes in successive annual iterations of the doubled CO_2 regional model run with interactive vegetation (RUN3).

Year	1	2	3	4	5	6	7	8
Change (%)	36.0	12.6	12.3	12.3	13.6	10.0	9.70	8.9

Another type of vegetation feedback occurs in the northeastern corner of the domain near the coast above 43°N, where a large area of evergreen taiga is replaced by desert and grassland. This coincides with pronounced extra cooling due to vegetation feedback in spring, autumn, and winter (Fig. 12), likely due to reduced snow masking by evergreen trees, which lowers wintertime albedos in the present simulation (e.g., Bonan et al. 1992).

In southern China, vegetation feedback produces small but uniform cooling of up to 0.5°C in winter, in exactly those regions where warm mixed forest replaces temperate deciduous forest (Figs. 2a,b), causing an increase in wintertime LAI. This might be due to the same basic deforestation mechanisms as for the northern cooling discussed earlier but in the opposite direction; however, the amplitudes are smaller and there is little change in the summer months.

Seasonal cycles of temperature change caused by vegetation feedback are shown for the three subregions in Fig. 13a. The strongest impacts occur in the northern region, where summer warming and winter cooling are pronounced. Late-spring warming in central China and winter cooling in southern China are also significant.

The effects of vegetation feedback on precipitation are more complicated and involve more factors than those for temperature. Maps of precipitation changes (RUN3 − RUN2, not shown) are somewhat chaotic, without large-scale structure. However, spatial averages for the three subregions (Fig. 13b) show coherent trends. In southern China, the effects of interactive vegetation feedback are largest in winter, with precipitation increases of 2%–4% from November to February and essentially no changes in summer. One possible reason for the additional winter precipitation might be that, with warm mixed forest replacing temperate deciduous forest in southern China, canopy roughness is larger in winter. In southern China most winter precipitation events are due to frontal activity, so mechanisms that trigger precipitation are important. By influencing the surface boundary layer and mechanical turbulence, larg-

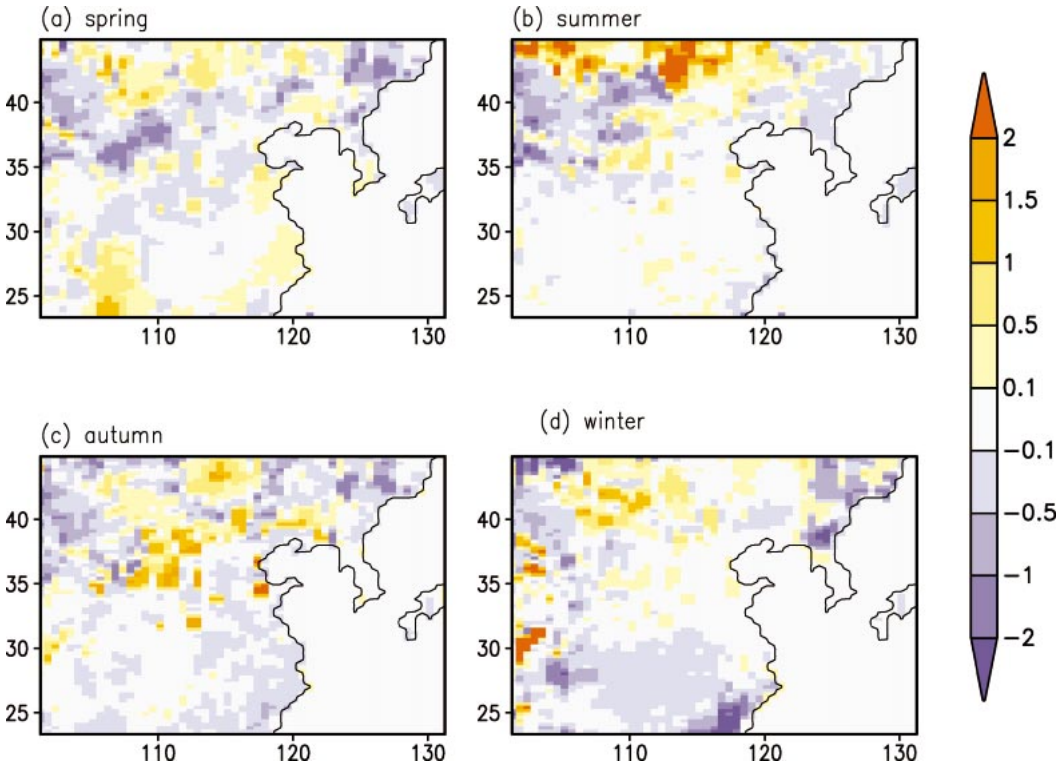

FIG. 12. Change in seasonal surface-air temperature (°C) due to vegetation feedbacks alone in the regional model under doubled CO_2 (RUN3 − RUN2): (a) spring (MAM), (b) summer (JJA), (c) autumn (SON), and (d) winter (DJF).

er wintertime canopy roughness in the interactive vegetation experiment (RUN3) could trigger more precipitation events than in RUN2.

A large increase (3%–4%) in precipitation is produced by vegetation feedback in August and September over northern China, coinciding with the main rainy season there. There are a number of complex processes that influence summer precipitation in northern China, including developing disturbances along the westerlies, local convective activity triggered by strong surface heating, and synoptic-scale cyclonic activity, and it is difficult to determine which processes are modified by interactive vegetation. However, we can seek some understanding empirically, by studying the correlations between changes in LAI, one of the basic vegetation indices, and changes in temperature and precipitation.

The spatial correlations over land between changes due to vegetation feedback alone (RUN3 − RUN2) in temperature, precipitation, and LAI are shown in Table 2. LAI changes correlate strongly with surface temperature, but with opposite signs depending on region and season. Sparser vegetation cover in northern China cools the land surface in winter, but warms it in summer. In southern China, however, denser vegetation cover tends to cool the surface in all seasons, with the winter correlation stronger than the summer. Clearly, vegetation feedbacks have opposite effects on surface temperature in northern and southern China, as discussed earlier in connection with Figs. 12 and 13. For LAI and precipitation, the correlation is higher in northern China in the warm months, reflecting strong interactions between vegetation and atmosphere there. The correlation in northern China between LAI and precipitation is smaller in the cold months than in the warm months, possibly because most large precipitation events occur in summer, and local evaporation contributes more than 10% to total precipitation (Chen et al. 2003a, 2003b, manuscript submitted to *J. Hydrometeor.*; Trenberth 1999), which makes surface feedbacks more important. In southern China, LAI and precipitation have little correlation, which is understandable since water vapor supply never limits precipitation there, and so triggering mechanisms for precipitation are more important.

7. Summary and conclusions

The importance of incorporating vegetation interactively into climate models has been appreciated since the 1980s. Earlier studies describe vegetation feedbacks through prescribing characteristic parameters in various land surface schemes such as the Biosphere–Atmosphere Transfer Scheme (BATS) of Dickinson et al. (1986, 1993), the Land Surface Transfer scheme (LSX) of Pollard and Thompson (1995), and the Land Surface

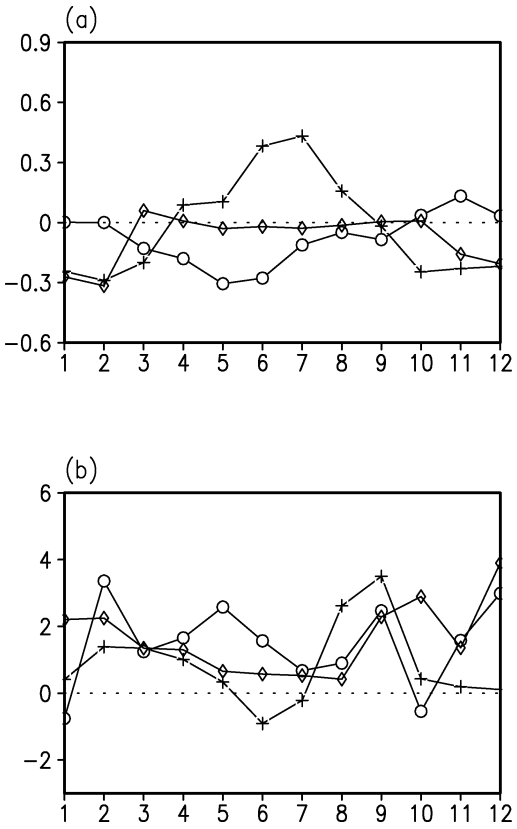

FIG. 13. Changes due to vegetation feedbacks alone in the regional model under doubled CO_2 (RUN3 − RUN2), over land for the three subregions shown in Fig. 1: (a) change in surface-air temperature (°C), (b) change in precipitation (%). Crosses are for northern China, circles for central China, and diamonds for southern China.

Model (LSM) of Bonan (1996). Interactive representations of ecosystem distribution in climate models have been undertaken by Foley et al. (1998), Dickinson et al. (1998), Lu et al. (2001), and Wang and Eltahir (2000) among others. In the current study, a coupled climate–soil–vegetation model is used to explore climate and ecosystem change under doubled CO_2 condition in East Asia, including ecosystem feedbacks on climate. One motivation for our focus on the East Asia monsoon region is that it is considered to be extremely sensitive to climatic and ecological perturbations (Ding 1994; Fu and Wen 1999).

Our climate version of the MM5 regional model simulates present-day climate in East Asia reasonably well. Correlation coefficients between model-simulated and observed surface-air temperatures are 0.95 and 0.84 for winter and summer, respectively. Mainly because of a cold bias in the large-scale GCM driving field, simulated temperatures are underestimated over the model domain. The observed characteristics of monsoon precipitation are well captured by the regional model. Biases in precipitation are partly due to the unrealistic position of the subtropical high and weak southwesterly winds in the large-scale GCM forcing, although shortcomings in the local physical schemes of the regional model itself may also contribute.

TABLE 2. Spatial correlation coefficients between changes in LAI, temperature, and precipitation for doubled CO_2 in the regional model due to vegetation feedbacks alone (RUN3 − RUN2), over land for the three subregions shown in Fig. 1. (L–T is the correlation coefficient between changes in LAI and temperature, and L–P is the correlation between changes in LAI and precipitation.)

	Cold months (Nov–Mar)		Warm months (May–Sep)	
	L–T	L–P	L–T	L–P
South	−0.62	0.08	−0.14	0.03
Central	0.3	0.14	−0.37	0
North	0.46	−0.13	−0.45	0.3

For the 2090's ''doubled CO_2'' experiment, the regional model predicts an overall increase of 23% in annual precipitation in northern China (mostly in coastal areas) and 21% in central China, but only 8% in southern China. The precipitation increase in northern and central China occurs mainly in the warm season. Surface heating caused by doubled CO_2 is weak in southern China without a distinct seasonal cycle. The strongest warming occurs in summer in northern China, with temperature increase of up to 4°C. The regional model also captures details on finer scales. For example, in some inland areas in northern China and adjacent Mongolia, spring and summer precipitation tends to decrease, contrary to the general tendency in northern China. Most of the changes due to doubled CO_2 discussed in this paper are associated with changes in the East Asian monsoon, which is intensified under doubled CO_2. Generally under doubled CO_2 the climate tends to be warmer and wetter, except for inland areas of northern China that tend to be warmer and drier.

Changes in vegetation patterns in response to a doubled CO_2 climate are significant in northern China and adjacent Mongolia, but less so in regions south of 40°N. Using the interactive vegetation model BIOME4, 36% of all land points in the model domain experience a change in vegetation type with doubled CO_2. In northern China, the area of forest is reduced by 14%, and shrub land, grassland, and desert areas increase by 8%, 1%, and 4%, respectively. Temperate deciduous forest expands due to warmer and wetter climate in limited coastal and central areas of northern China around 40°N. Larger changes occur in northern inland areas, where water supply is more critical than temperature for vegetation growth, and deserts and shrub land expand over widespread areas due to warmer and drier climate. In general, grassland and shrubland expand at the expense of forest, and desert expands at the expense of grassland and forest. These inland areas of northern China experience particularly large changes and ecosystem deterioration, with forest declining by 14% and desert increasing by 4% under doubled CO_2, suggesting that this region is ecologically sensitive and vulnerable to climate change.

Feedbacks of vegetation on climate occur with distinct seasonal and spatial patterns. Over northern China, they intensify the inland warming trend caused by doubled CO_2 in summer, but tend to cool the surface in the winter. As discussed in section 6b, this is consistent with deforestation feedbacks seen in other GCM simulations, as reduced forest canopy intercepts less rainfall causing more runoff and drying. In southern China, vegetation feedbacks cool the surface in winter but have almost no effect in other seasons. As discussed in section 6b, this is probably due to increased canopy roughness of warm mixed forest replacing temperate deciduous forest, producing more precipitation events and cooling in winter. Feedbacks of vegetation on precipitation are stronger in the winter in southern China and in August–September in northern China, causing increases of more than 3% in both cases. Again, northern China experiences the strongest effects of vegetation feedback on temperature (most months) and precipitation (rainy season), indicative of large ecosystem sensitivity and vulnerability.

Significant uncertainties remain in the model system that require better understanding and improvement. First, the use of an equilibrium vegetation model neglects transient lags of the vegetation response to changing climate, although these might well affect vegetation and climate change in the coming decades. The lack of transient vegetation dynamics in our model also fails to capture interactions with natural variability on interannual and interdecadal scales. Second, biases in the large-scale GCM forcing as well as in imperfect local physics in the regional model also cause significant uncertainties in evaluating climate and ecosystem change. Last, since climate change and ecosystem evolution are slow, gradual processes, the lack of long-term observational records for the East Asian region hampers validation and interpretation of model results.

Acknowledgments. Constructive suggestions by two anonymous reviewers are greatly appreciated. This work was funded in part by the National Aeronautics and Space Administration Grant EOS-NAG5-4553 and made use of supercomputing resources supported by National Science Foundation Grant PMESH-ATM 0000545.

REFERENCES

Bonan, G. B., 1996: A land surface model (LSM 1.0) for ecological hydrological and atmospheric studies: Technical description and user's guide. NCAR Tech. Note 417, 150 pp.

——, D. Pollard, and S. L. Thompson, 1992: Effects of boreal forest vegetation on global climate. *Nature,* **359,** 716–718.

Boville, B. A., and P. G. Gent, 1998: The NCAR Climate System Model, version one. *J. Climate,* **11,** 1115–1130.

Briegleb, B. P., 1992: Delta–Eddington approximation for solar radiation in the NCAR Community Model. *J. Geophys. Res.,* **97,** 7603–7612.

Cai, Z., and M. Zhang, 1978: Analysis of excessively heavy rain between Inner Mongolia and Shanxi Province. *Selected Papers on Rainstorm,* Z. Baozhen, Ed., Jilin People's Press, 138–146.

Charney, J. G., 1975: Dynamics of deserts and droughts in Sahel. *Quart. J. Roy. Meteor. Soc.,* **101,** 193–202.

Chen, M., D. Pollard, and E. J. Barron, 2003a: Comparison of future climate change over North America simulated by two regional models. *J. Geophys. Res.,* **108,** 4348, doi:10.1029/2002JD002738.

——, ——, and ——, 2003b: Hydrologic processes in China and their association with summer precipitation anomalies. *J. Hydrometeor.,* submitted.

Claussen, M., 1994: On coupling global biome models with climate models. *Climatic Res.,* **4,** 203–221.

——, 1997: Modeling bio-geophysical feedback in the African and Indian monsoon region. *Climate Dyn.,* **13,** 247–257.

Costa, M. H., and J. A. Foley, 2000: Combined effects of deforestation and doubled atmospheric CO_2 concentrations on the climate of Amazonia. *J. Climate,* **13,** 18–34.

Cramer, W., 2002: Biome models. *The Earth System: Biological and Ecological Dimensions of Global Environmental Change,* H. Mooney and J. Canadell, Eds., Wiley, 166–171.

Davies, H. C., and R. E. Turner, 1977: Updating prediction models by dynamical relaxation: An examination of the technique. *Quart. J. Roy. Meteor. Soc.,* **103,** 225–245.

Dickinson, R. E., A. Henderson-Sellers, P. J. Kennedy, and M. F. Wilson, 1986: Biosphere–Atmosphere Transfer Scheme (BATS) for the NCAR Community Climate Model. NCAR/TN-275+STR, 69 pp.

——, ——, and ——, 1993: Biosphere–Atmosphere Transfer Scheme (BATS) version 1E as coupled to the NCAR Community Climate Model. NCAR/TN-387+STR, 72 pp.

——, M. Shaikh, R. Bryant, and L. Graumlich, 1998: Interactive canopies for a climate model. *J. Climate,* **11,** 2823–2836.

Ding, Y., 1994: *Monsoons over China.* Kluwer Academic, 419 pp.

Dudhia, J., 1989: Numerical study of convection observed during the winter monsoon experiment using a mesoscale two-dimensional model. *J. Atmos. Sci.,* **46,** 3077–3107.

Ferranti, L., J. M. Slingo, T. N. Palmer, and B. J. Hoskins, 1999: The effects of land-surface feedbacks on monsoon circulation. *Quart. J. Roy. Meteor. Soc.,* **125,** 1527–1550.

Foley, J. A., S. Levis, I. C. Prentice, D. Pollard, and S. L. Thompson, 1998: Coupling dynamic models of climate and vegetation. *Global Change Biol.,* **4,** 561–579.

Fu, C. B., and G. Wen, 1999: Variation of ecosystem over East Asia in association with seasonal interannual and decadal monsoon climate variability. *Climatic Change,* **43,** 477–494.

Grell, G. A., J. Dudhia, and D. R. Stauffer, 1994: A description of the fifth-generation Penn State/NCAR Mesoscale Model (MM5). NCAR/TN-398+STR, 117 pp.

Haxeltine, A., and I. C. Prentice, 1996: BIOME3: An equilibrium terrestrial biosphere model based on ecophysiological constraints, resource availability and competition among plant functional types. *Global Biogeochem. Cycles,* **10,** 693–709.

Hoffmann, W. A., and R. B. Jackson, 2000: Vegetation–climate feedbacks in the conversion of tropical savanna to grassland. *J. Climate,* **13,** 1593–1602.

Hong, S. Y., and H. L. Pan, 1996: Non-local boundary layer vertical diffusion in a medium-range forecast model. *Mon. Wea. Rev.,* **124,** 2322–2339.

Kalnay, E., and Coauthors, 1996: The NCEP/NCAR 40-Year Reanalysis Project. *Bull. Amer. Meteor. Soc.,* **77,** 437–471.

Kaplan, J. O., 2001: Geophysical applications of vegetation modeling. Ph.D. thesis, Lund University, 114 pp.

Lean, J., and P. R. Rowntree, 1997: Understanding the sensitivity of a GCM simulation of Amazonian deforestation to the specification of vegetation and soil characteristics. *J. Climate,* **10,** 1216–1235.

Leemans, R., and W. Cramer, 1991: The IIASA climate database for mean monthly values of temperature, precipitation and cloudiness of a global terrestrial grid. IIASA Research Rep. RR-91-18, 61 pp.

Lu, L., R. A. Pielke, and G. L. Liston, 2001: Implementation of a two-way interactive atmospheric and ecological model and its

application to the central United States. *J. Climate,* **14,** 900–919.

Meehl, G. A., 1994: Influence of land surface in the Asian summer monsoon: External condition versus internal feedbacks. *J. Climate,* **7,** 1033–1048.

New, M., M. Hulke, and P. Jones, 1999: Representing twentieth century space–time climate variability. Part I: Development of a 1961–90 mean monthly terrestrial climatology. *J. Climate,* **12,** 829–856.

Ni, J., 2001: Carbon storage in terrestrial ecosystems of China: Estimates at different spatial resolution and their response to climate change. *Climatic Change,* **49,** 339–358.

Pollard, D., and S. L. Thompson, 1995: Use of a land surface transfer scheme (LSX) in a global climate model: The response to doubling stomatal resistence. *Global Planet. Change,* **10,** 129–161.

——, J. C. Bergengren, L. M. Stillwell-Soller, B. J. Felzer, and S. L. Thompson, 1998: Climate simulations for 10000 and 6000 years BP using the GENESIS global climate model. *Paleoclimates,* **2,** 183–218.

Shukla, J., and Y. Mintz, 1982: Influence of land-surface evaporation on earth's climate. *Science,* **214,** 1498–1501.

Tao, S. Y., 1979: *Heavy Rainfall in China.* Science and Technology Press, 578 pp.

Texier, D., and Coauthors, 1997: Quantifying the role of biosphere–atmosphere feedbacks in climate change: Coupled model simulations for 6000 BP and comparisons with palaeodata for northern Eurasia and northern Africa. *Climate Dyn.,* **13,** 865–882.

Thompson, S. L., and D. Pollard, 1997: Greenland and Antarctic mass balance for present and doubled atmospheric CO_2 from the GENESIS version 2 global climate model. *J. Climate,* **10,** 871–900.

Trenberth, K., 1999: Atmospheric moisture recycling: Role of advection and local evaporation. *J. Climate,* **12,** 1368–1381.

Tsvetsinskaya, E. A., and L. O. Mearns, 2001: Investigating the effects of seasonal plant growth and development in three-dimensional atmospheric circulation. Part I: Simulation of surface fluxes over growing season. *J. Climate,* **14,** 692–709.

Wang, G. L., and E. A. B. Eltahir, 2000a: Biosphere–atmosphere interactions over West Africa. I: Development and validation of a coupled dynamic model. *Quart. J. Roy. Meteor. Soc.,* **126,** 1239–1260.

——, and ——, 2001b: Biosphere–atmosphere interactions over West Africa. II: Multiple climate equilibria. *Quart. J. Roy. Meteor. Soc.,* **126,** 1261–1280.

Webster, P. J., and S. Yang, 1983: Mechanisms of monsoon low-frequency variability: Surface hydrological effects. *J. Atmos. Sci.,* **40,** 2110–2124.

Xie, P., and P. A. Arkin, 1996: Analyses of global monthly precipitation using gauge observations, satellite estimates, and numerical model predictions. *J. Climate,* **9,** 840–858.

Zeng, N., and J. D. Neelin, 2000: The role of vegetation–climate interaction and interannual variability in shaping the African savanna. *J. Climate,* **13,** 2665–2670.